Computers in Biology and Medicine 106 (2019) 65–70

Contents lists available at ScienceDirect

Computers in Biology and Medicine

journal homepage: www.elsevier.com/locate/compbiomed

Motor unit innervation zone localization based on robust linear regression analysis

Jie Liu[a,b,*], Sheng Li[c,f], Faezeh Jahanmiri-Nezhad[a,d], William Zev Rymer[a,e], Ping Zhou[c,f]

[a] Sensory Motor Performance Program, Shirley Ryan AbilityLab, Chicago, United States
[b] Kay Mounting Service Ltd, London, United Kingdom
[c] Department of Physical Medicine and Rehabilitation, University of Texas Health Science Center at Houston, Houston, United States
[d] Department of Bioengineering, University of Illinois at Chicago, Chicago, United States
[e] Department of Physical Medicine & Rehabilitation, Northwestern University, Chicago, United States
[f] TIRR Memorial Hermann Research Center, Houston, TX, United States

ARTICLE INFO

Keywords:
Innervation zone (IZ)
Motor unit action potential (MUAP)
Robust linear regression

ABSTRACT

With the aim of developing a flexible and reliable procedure for superficial muscle innervation zone (IZ) localization, we proposed a method to estimate IZ location using surface electromyogram (EMG) based on robust linear regression. Regression lines were used to model the bidirectional propagation pattern of a single motor unit action potential (MUAP) and visualize the trajectory of the MUAP propagation. IZ localization was performed by identifying the origin of the bidirectional MUAP propagation. Robust linear regression and MUAP peak detection, combined with propagation phase reversal identification, may provide an efficient way to estimate IZ location. Our method offers high resolution in locating IZs based on simulation studies and experimental tests. Furthermore, our method is flexible and may also be applied using a relatively small number of EMG channels. A comparative study of the proposed method with the cross-correlation method for IZ localization was conducted. The results obtained with simulated MUAPs and measured spontaneous MUAPs in the biceps brachii muscle in six subjects (four males and two females, 57 ± 10 years old) with amyotrophic lateral sclerosis (ALS). Our method achieved estimation performance comparable to that obtained by using the cross-correlation method but with higher resolution. This study provides an accurate and practical method to estimate IZ location.

1. Introduction

Recording of muscle activity using surface electrode array electromyogram (EMG) technology is a useful technique that provides valuable information about muscle/motor unit anatomy and function [1–8]. Electrode array EMG can be used to locate the innervation zone (IZ) of a muscle. IZ localization has long been a question of great interest in the EMG studies and remains under active research. A considerable amount of literature has been published on IZ localization. For example, the optimal site of botulinum toxin (BT) injection is the muscle IZ and accurate local injection of BT into spastic muscle IZ is one approach to the treatment of spasticity [1,9–11]. Electrode array EMG can also be used to study individual motor unit properties, including their IZ. In neuromuscular diseases, loss of motoneurons and motor unit remodelling may result in the reorganization of the IZ [12]. The study of the motor unit IZ may provide important information about denervation and reinnervation processes in conditions such as amyotrophic lateral sclerosis (ALS) [13].

The identification of the motor unit or muscle IZ using surface EMG signals detected with a linear array or a 2-dimensional electrode grids has been extensively discussed in the literature [1,14–25]. Thus far, IZ locations of recognized motor units using linear electrode arrays have been estimated using cross-correlation, minimum amplitude (root mean square), and maximum center frequency (mean frequency) criteria [24] and interpolated image based methods [26,27]. However, there is currently no practical standard clinical procedure for rapid localization of the IZ. Especially, many laboratories do not have access to a linear electrode array, this indicates a need to estimate the IZ by manually configuring the electrode arrangements.

The goal of the current study was to develop a quick and convenient method for automatic detection of motor unit IZ based on robust linear regression analysis. The performance of the proposed method was assessed with both simulation and experimental studies. As the cross-correlation based method is more accurate for estimating IZ location in

* Corresponding author. Kay Mounting Service Ltd, Rangemoor Industrial Estate Bernard Rd, London, N15 4NE, United Kingdom.
E-mail address: jie.liu2009@gmail.com (J. Liu).

https://doi.org/10.1016/j.compbiomed.2019.01.007
Received 26 August 2018; Received in revised form 13 January 2019; Accepted 13 January 2019
0010-4825/

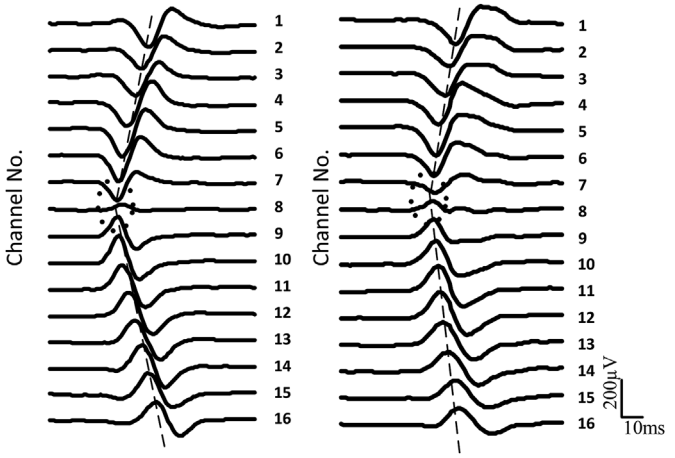

Fig. 1. Examples of experimental individual MUAPs detected by a linear array. Sixteen single differential (SD) surface EMG signals over a 0.10 s epoch are numbered from distal to proximal locations of the biceps brachii of a healthy adult. The dashed line represents MUAP propagation. The dotted circle indicates the IZ location, estimated by the operator (Left: channel 8; Right: between channel 7 and channel 8).

comparison with other methods, such as the lowest amplitude and highest mean frequency criteria based methods [24], the performance of the linear regression analysis was further compared with the cross-correlation based analysis for motor unit IZ estimation. Furthermore, given that many clinical laboratories do not have access to electrode array technology [24], with the aim of decreasing the number of recording channels, we also tested the regression method for accurate IZ estimation using surface EMG signals obtained from relatively few channels instead of using signals obtained from all available channels of the electrode array.

2. Methods

2.1. IZ estimation using linear regression

Fig. 1 shows examples of experimental motor unit action potential (MUAP) propagation along muscle fibers, detected by an electrode array. The visual identification of motor unit IZ was determined using the following criteria: (a) the bipolar action potentials have opposite polarities on both sides of the motor unit IZ; (b) a clear MUAP propagation pattern can be observed from the IZ to proximal and distal muscle tendons; (c) the channel located closest to the center of the motor unit IZ results in action potentials with much lower amplitude than the channels between the IZ and the tendon. Thus, the location of the motor unit IZ was visually identified as the origin from which bipolar MUAPs propagate in opposite directions. Clear MUAP propagation was observed between the IZ and the muscle tendons. The IZ location can be identified as the origin of the bidirectional propagation of a single MUAP along the muscle fibers on multi-channel electrodes.

The IZ location was detected by visual search for a minimal amplitude channel and/or phase reversal in the single differential (SD) signal. When the minimal amplitude channel was between two SD channels showing phase reversal, it was assumed to be the location of the IZ (Fig. 1, left panel). Conversely, when two adjacent electrodes showed phase reversal, the IZ was assumed to be located between the two channels, (Fig. 1, right panel).

The MUAP propagation in the two different directions can be represented by applying regression lines to the identified MUAP peaks after identifying the reversal phases. Robust linear regression is an alternative to ordinary least squares regression and provides much better regression coefficient estimates when outliers are present in the data. Basically, outliers infringe the assumption of normally distributed residuals in least squares regression and lead to serious distortions in the estimated coefficients. A four-stage IZ estimation algorithm using MUAPs recorded simultaneously on multiple channels was developed based on robust linear regression to estimate motor unit IZ location.

1. The positive and negative peaks of MUAP signals were identified from all the measured signals from the array channels. All the channels were from one side if the positive peak was before the negative peak. In contrast, other channels were from the other side if the negative peak was before the positive peak. The program was inspecting signals for ensuring the positioning of the examined channels so that both sides from the IZ were covered by the channels.
2. The MUAP propagation phase reversal, based on MUAP polarity changes, was determined based on the positive peak lagging behind the negative peak by a few milliseconds.
3. Two straight lines were fit the peaks obtained from the same side from the IZ using linear regression. The most widely used method for fitting a regression line is the method of least-squares. By contrast, the weighted least squares method is a feasible alternative robust to outliers. Previous studies have demonstrated that an iteratively reweighted least squares (IRLS) approach minimizes the influence of outliers, thus reducing confidence intervals relative to the standard ordinary least squares method [28,29]. Therefore, we used IRLS with a bisquare weighting function to obtain the regression lines.
4. The IZ of the motor unit was located at the intersection of the two linear regression lines.

In order to determine two straight regression lines respectively, MATLAB (Version R2008a, MathWorks Inc., Natick, Massachusetts) built-in function *robustfit* was used to perform IRLS regression. A regular least-square fitting was first performed. The residuals of the fitting R were calculated after the fitting. Iterations were then performed until there is convergence of the residual. The weights W for the next iteration were determined by Tukey's bisquare function:

$$W = \begin{cases} (1 - K^2)^2 & when\ abs(K) < 1 \\ 0 & when\ abs(K) \geq 1 \end{cases} \quad (1)$$

where

$$K = \frac{\mathrm{R}}{4.685 \times \left(\frac{\mathrm{MAD}}{0.6745}\right) \times \sqrt{1-\mathrm{h}}} \quad (2)$$

R is the vector of residuals from the previous iteration, MAD is the median absolute deviation of the residuals from their median, and h is the vector of leverage values from a least-square fit to identify observations with unusual or outlying values.

To estimate the source of the propagation of MUAPs, two regression lines are required. Furthermore, recordings from at least two channels are required for determining each regression line. In addition to testing the method with all channels of the array, the method was also tested based on recordings from 4 array channels.

2.2. Simulation database

A validation study was conducted to evaluate the performance of the proposed method using simulated MUAPs collected via a linear electrode array where the IZ was known *a priori*. In general, a single fiber action potential (SFAP) can be modeled as a convolution of bioelectrical source and filtering functions [30,31]. According to previous work [32,33], the SFAP at the recording point is expressed as

$$\phi(t, r, d) = k \cdot s(t) * [h_l(t, r, d, t_l) + h_r(t, r, d, t_r)] \quad (3)$$

where $k = \frac{1}{2}\frac{\sigma_i \theta^2}{4\sigma_e}$ is a constant that accounts for conductivities and the

fiber radius to velocity constant ratio, in which $\theta = \frac{\alpha}{v}$ can be considered constant, and in the order of $0.2(\mu m)/(m/s)$[34],

$$s(t) = \sum_{1}^{3} b_i\left(c_i\left(\frac{t}{2} - g_i\right)\right)\cdot e^{c_i\left(\frac{t}{2} - g_i\right)} \tag{4}$$

where $b_1 = 51$, $b_2 = 72$, $b_3 = 18$, $c_1 = -64$, $c_2 = -28.41$, $c_3 = -11.09$, $g_1 = 0.54$, $g_2 = 0.66$, $g_3 = 0.86$ [30].

$$h_l(t, r, d, t_l) = \begin{pmatrix} 0 & t < 0 \\ h\left(t + \frac{d}{v}\right) & 0 \le t \le t_l \\ 0 & t > t_l \end{pmatrix} \tag{5}$$

$$h_r(t, r, d, t_r) = \begin{pmatrix} 0 & t < 0 \\ h\left(t - \frac{d}{v}\right) & 0 \le t \le t_r \\ 0 & t > t_r \end{pmatrix} \tag{6}$$

where $t_l = \frac{l_l}{v}$, $t_r = \frac{l_r}{v}$ and. $h(t) = \frac{t}{\left(t^2 + \left(\frac{r}{v}\right)^2\right)^{\frac{3}{2}}}$

In the above equations, r is fiber depth underneath the recording electrode; d is axial distance from the motor point to the recording electrode; l_r and $l_l$are distances from the motor point to the right and left fiber terminations, respectively; σ_i and σ_e are intracellular and extracellular conductivities; a is fiber radius; v is conduction velocity.

Using the model of SFAP based on the convolution of a source and a tissue filter, surface MUAPs were simulated by summing the resulting multiple SFAPs [32,33]. The dispersion limits were chosen to model a typical motor unit of the brachial biceps muscle to account for individual fiber differences [35]. These parameters were chosen to model surface EMG measurements from the biceps muscle using a linear electrode array in single differential (SD) mode [35]. A summary of the physiological parameters is given in Table 1, with all dispersions randomly generated according to a uniform distribution. Electrodes with 5 mm inter-electrode distance were assumed to be placed along the length of the biceps which extended from −30 mm to +50 mm and −32.5 mm to +47.5 mm with respect to the center of the simulated motor unit IZ. The duration of each simulation was 100 ms.

To simulate MUAPs with different signal-to-noise ratio (SNR) levels, an independently generated zero-mean white Gaussian noise was artificially added to the simulated clean MUAPs. The standard deviation of the noise was determined by different SNRs (20, 15, 10, 8, 5, 3, 2 and 1 dB) of simulated MUAPs. For each SNR, 50 MUAPs were generated. All the simulated signals were sampled at 2000 Hz and processed with a 4th order Butterworth band-pass filter at 20–500 Hz.

We simulated two types of experimental MUAP recordings. The first type represents a MUAP recording where the IZ is detected at one channel (Fig. 1 left panel). The second type represents a MUAP recording where the IZ is detected between two adjacent channels (Fig. 1 right panel). Both groups of simulated MUAPs were used to examine the IZ estimation performance of the proposed method under different conditions.

Table 1
Physiological parameters of muap simulation.

Physiological Parameter	Value
Number of MU M	50
Number of fibers/MU N	[50, 100]
Distance from motor point of a fiber to its left termination l_l	−220 ± 5 mm
Distance from motor point of a fiber to its right termination l_r	−190 ± 5 mm
Motor point dispersion m_d	0 ± 2 mm
Vertical depth of motor units d_v	[5,20] ± 5 mm
Horizontal alignment of motor units d_e	[-5,5] ± 5 mm
Limb radius R_l	40 mm
Conduction velocity v	4 m/s
Source duration Ts	3 ms

Table 2
Demographic information of the ALS subjects.

Subject #	Age (year)	Gender	Diagnosis
1	56	M	Definite
2	71	M	Probable with Lab Support
3	46	M	Definite
4	52	F	Definite
5	48	M	Definite
6	68	F	Definite

2.3. Experimental database

The proposed motor unit IZ estimation method was also tested with experimental recordings. Six subjects with " definite ALS ″ or " probable ALS with laboratory support " based on El Escorial criteria participated [36]. Table 2 provides demographic information about the ALS subjects; four males and two females, aged 46–71 years (average age 57 ± 10 years). The study was approved by the local Human Ethics Studies Committee. Spontaneous biceps brachii muscle activity was recorded with the elbow partially flexed and forearm in semi-pronation. The subject was asked to keep the muscle as relaxed as possible. A 20-silver bar linear electrode array (10 mm long and 1 mm width bars, 5 mm inter-electrode distance) was used for surface EMG recording. A reference electrode was located on the olecranon. The array was placed longitudinally over the biceps between the proximal to distal tendon junctions. The EMG signals were amplified by the Refa EMG system (TMS International BV, The Netherlands), sampled at 2000 Hz per channel, and band pass filtered (20–500 Hz). The waveform information from multiple channels was used to classify spontaneous action potentials from different motor unit origins. For each identified motor unit origin, the action potential template was obtained by averaging those action potentials clustered to the origin with confidence. Then, the monopolar action potentials were processed by subtracting each pair of adjacent bars along the muscle fibers. The three most proximal and distal bars were excluded from the analysis because they were close to the tendons and sometimes resulted in noisy signals. The remaining 17 bars resulted in 16 channels of spatially filtered bipolar signals.

2.4. Comparison with cross-correlation method

All data processing was performed offline using MATLAB. Signals were processed by three different methods for automatic detection of motor unit IZ. (1) Cross correlation method; This method calculates the cross correlation of signals from adjacent channels of the linear electrode array. When the IZ is detected at a channel, the correlation of this channel with other channels is low. The two channels that had the lowest peak cross correlation value between the bipolar signals were first determined. The IZ was then estimated to be located between these two channels; (2) linear regression based on data from all 16 channels; (3) linear regression based on data from 4 channels. The effect of the estimation method on IZ estimation performance was evaluated.

3. Results

3.1. Results from simulated surface EMG signals

Fig. 2 depicts examples of applying the proposed method to representative simulated MUAPs for IZ estimation. It was observed that the linear regression based method was able to estimate IZ location as being located on one channel (Fig. 2b) or between two adjacent channels (Fig. 2c).

Fig. 3 demonstrates an example of applying the proposed method compared to the cross-correlation method for IZ estimation based on simulated MUAPs. The maximum cross-correlation coefficients between adjacent channels are shown. Both the cross correlation and the robust

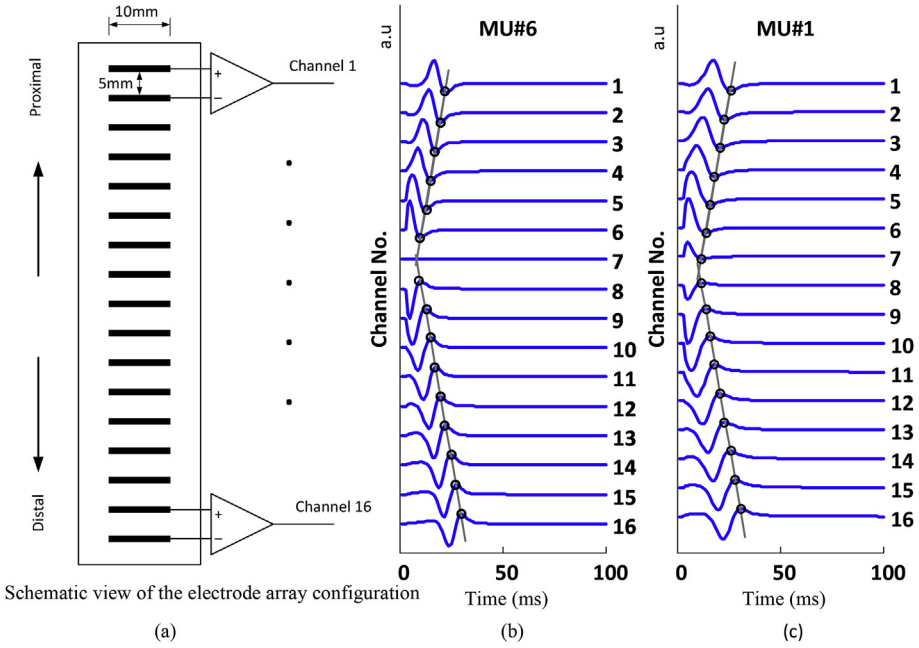

Fig. 2. Examples of IZ location determined by the intersection of two linear regression lines which represent the estimated trajectories of bidirectional propagating potentials. The circles indicate the identified MUAP peaks measured on 16 SD channels. Gray lines are resultant regression lines and represent MUAP propagation. The intersection point of the two regression lines indicates the estimated IZ location (b: channel 7, c: between channel 7 and channel 8).

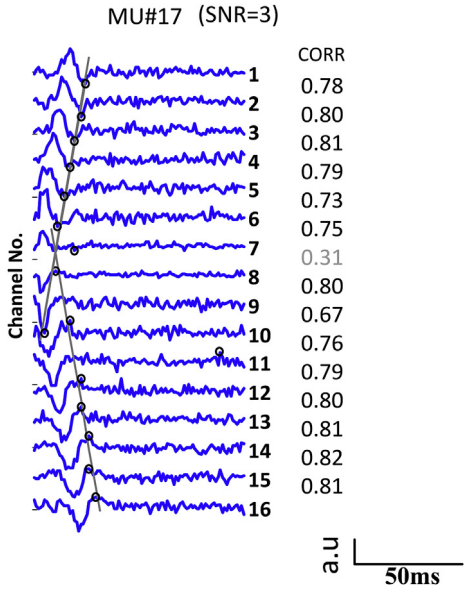

Fig. 3. The MUAP and the corresponding IZs estimated by the robust linear regression method and the cross-correlation method. The MUAP obtained from two adjacent channels are cross-correlated. The peak cross-correlation coefficients obtained from adjacent channels are presented and the minimum value corresponds to the IZ (0.31, gray).

regression methods achieved the same estimation.

Table 3 presents a performance comparison of the two IZ estimation methods. In summary, the cross-correlation based method estimated the location of the IZ in 100% (800 out of 800 MUAPs) of the cases regarding the overall accuracy. The robust linear regression based method estimated the location of the IZ in 99.8% (798 out of 800 MUAPs) of the cases. In order to decrease the number of recording channels, we also compared the performance achieved by using 16 channels versus 4 channels in terms of the robust linear regression method. The normality of distribution of accuracies of all the examined SNRs was examined by using the Lilliefors test, revealing that the accuracies are different from the normal distribution. The mean estimation accuracies of the RLR method and the CORR method were not

Table 3
Estimation accuracy of IZ location (Unit: %).

SNR	Type I		Type II	
	RLR	CORR	RLR	CORR
1	100(100)	100	98(98)	100
2	100(100)	100	98(98)	100
3	100(100)	100	100(100)	100
5	100(100)	100	100(100)	100
8	100(100)	100	100(100)	100
10	100(100)	100	100(100)	100
15	100(100)	100	100(100)	100
20	100(100)	100	100(100)	100

*RLR and CORR: Accurate estimation of IZ location obtained from the robust linear regression method, the cross-correlation method, respectively. Numbers in parenthese show the estimation accuracy by using the RLR method with only 4 channels collected from the opposite sides of the IZ.

significantly different from each other (a Kruskal-Wallis (nonparametric one-way ANOVA) test, $p > 0.1$). The robust linear regression method achieved robust performance with varying SNR levels like the cross-correlation method. Furthermore, the resolution achieved by linear regression was not limited by the inter-electrode distance of the linear electrode array, which was higher than that obtained by the cross-correlation method.

Table 4 shows the comparison of running times for IZ estimation using the RLR and CORR methods. Note that the time cost for

Table 4
Averaged running times (mean ± SD in milliseconds) of the RLR and CORR methods at each examined SNR.

SNR	CORR	RLR
1	3.8 ± 1.5	2.2 ± 0.7
2	3.1 ± 0.3	1.8 ± 0.6
3	3.3 ± 0.9	2.0 ± 0.7
5	3.2 ± 0.6	1.7 ± 0.6
8	4.0 ± 1.6	2.3 ± 1.1
10	3.2 ± 0.7	1.7 ± 0.4
15	2.9 ± 0.3	1.5 ± 0.3
20	3.1 ± 0.3	1.5 ± 0.3
Averaged (Mean ± SD)	3.3 ± 0.4	1.8 ± 0.3

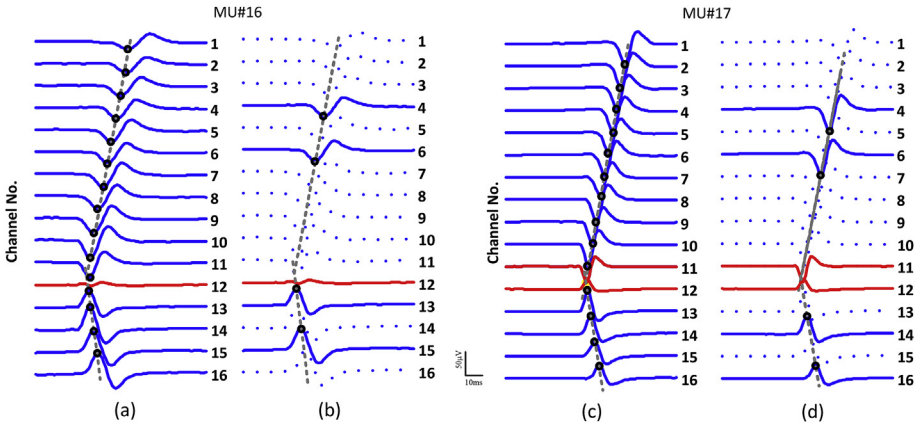

Fig. 4. Examples of experimental MUAPs and the corresponding IZs estimated by the proposed method. The IZs were estimated by using 16 SD surface EMG signals (a) and (c) or four SD surface EMG signals (b) and (d). The circles indicate the identified positive and negative MUAP peaks. The gray dotted lines are resultant regression lines and represent MUAP propagation. The intersection point of the two regression lines indicates the estimated IZ location. (Left panel (a) and (b): channel 12; Right panel (c) and (d): between channel 11 and channel 12).

identifying action potentials from single units were not considered. The mean time was averaged across 200 MUAP signal segments at each tested SNR. The analyses were performed with a custom-made MATLAB program. It took 3.3 ± 0.4 ms to estimate the IZ by using a 100 ms simulated MUAP recording by the cross-correlation method. In contrast, our method is computationally efficient. it took 1.8 ± 0.3 ms to estimate the IZ of the same signal by using our method (performed on a 2.5-GHz Intel Core i5 based PC using a 64-bit Windows 10 operating system with 8-GB Memory). The RLR method is statistically superior to the CORR method at each examined SNR in terms of running time (Kruskal-Wallis test, $p < 0.01$)).

3.2. Testing on experimental surface EMG signals

The spontaneous action potentials collected from biceps brachii muscle of six ALS subjects were used to extract the motor unit for each identified motor unit origin. We have 40 experimental MUAPs in total. A comparative study of the proposed method and the cross-correlation method for IZ localization was conducted with measured spontaneous MUAPs in the biceps brachii muscle. For experimental MUAPs, each individual IZ was estimated visually as a standard. Fig. 4 demonstrates examples of applying the proposed method to experimental MUAPs for IZ estimation. The proposed method was able to estimate the IZs accurately. Using visual inspection of the experimental signals as a standard, the estimation performance of the two methods was further examined. The cross-correlation based method estimated the location of the IZ in 92.5% (37 out of 40 MUAPs) of the cases. The proposed method estimated the location of the IZ in 90.0% (36 out of 40 MUAPs) of the cases. Similarly, we also compared the performance of the robust linear regression method using 16-channel and 4-channel recordings collected from the opposite sides of the IZ. We found that the proposed method was able to estimate the location of the IZ by using all 16 channels (36 out of 40 MUAPs) and 4 channels (34 out of 40 MUAPs).

4. Discussion

This study investigated a robust linear regression method for motor unit IZ localization using a linear electrode array. The performance of the proposed method was compared with the cross-correlation method. Compared with cross correlation methods, the method introduced in the current study has several advantages including high resolution, less sensitivity to the effects of inter-electrode recording distance. The method based on robust linear regression analysis can give the location of IZ with high resolution for a MUAP recording where the IZ is between two adjacent channels (Fig. 1 right panel). The estimated IZ achieved by using the cross-correlation method, is only estimated between the two channels and without a specified point, thus the estimated IZ is sensitive to inter-electrode recording distance.

Our method successfully located the IZ using a small subset of the channel array less than other methods, thus further decrease the computation load for IZ localization. We observed that our method estimated IZs using only 4-channel bipolar EMG signals aligned with the muscle fiber direction (Fig. 4). Theoretically, the four channel EMG signals need to be collected from the opposite sides of the IZ. The 4-channel configuration is easy to apply. Because the identified IZ will not lie between the two set of channels, the method can determine the wrong placement of the electrodes on only one side. Thus our findings are of practical importance because many laboratories do not have access to a linear electrode array. In particular, combining manually configuring the electrode arrangements and the proposed method would allow for flexible and reliable procedures for superficial muscle IZ localization.

The present work focused on motor unit IZ localization, and the performance of the proposed method was evaluated with both simulation and experimental recordings of spontaneous EMG from ALS subjects. The method is also possibly applicable to global muscle innervation estimation following motor nerve stimulation, which results in the near simultaneous activation of the motor units. For example, the proposed method can also be applied to estimate IZ location based on reconstructed evoked compound muscle action potentials (CMAPs) [37] particularly for patients who have poor motor control, after removing the stimulation artifacts using a method presented in our previous research [38]. In terms of locating the IZs, one main difference between evoked CMAPs and MUAPs obtained from spontaneous surface EMG recordings is that stimulus artifacts are likely to contaminate the CMAPs when stimulation and recording electrodes are close [38]. In this case, the linear regression method in conjunction with the stimulus artifact suppression proposed in our previous study [38] could be applied to evoked CMAPs to estimate IZs. This combined approach may potentially lead to practical EMG guided botulinum toxin injection to reduce muscle tone [1,9–11].

Our method with further improvements may be applied to different types of signals including motor units decomposed from the surface EMG interference pattern. For example, our method can possibly be applied to interference EMG recordings when the delay between two adjacent channels is computed based on the cross correlation of the signals from the two channels. It is worth noting that in cases which demonstrate multiple IZs, this approach may still result in accurate IZ estimations if the MUAPs from different motor units are decomposed successfully and essential criteria for the segmentation of recording channels are carefully considered.

Several limitations of the proposed method need to be acknowledged. First, this method unlikely applies when end-of-fiber effect is present and far-field potentials is the dominant component of the detected surface signal [39,40]. Second, this method does not apply to boundary conditions, when there is none or only one potential propagating towards either ending of the muscle fiber [26]. Third, because we used a one-dimensional linear electrode array, the medial–lateral

positioning of the IZ was not accounted for. Application of two-dimensional electrode arrays would help identify IZs of more lateral or medial motor units, thus being able to offer information about motor unit IZ distribution of the whole muscle [22,41]. The electrode was aligned in parallel with the fiber direction in this study. It is noteworthy that it is challenging to find a clinically feasible method for IZ localization that is applicable to all muscles due to muscle-specific diffuse distribution of motor endplates. Further studies are therefore required to determine the most appropriate method for muscle-specific IZ localization, particularly in muscles with in-depth pinnate (e.g. gastrocnemius [42,43]) and skin parallel-fibered (e.g. vastii [40]) architectures.

5. Conclusions

This project was undertaken to estimate motor unit IZ based on robust linear regression analysis. This study has shown that this method can locate the IZ using a small channel subset (4 channels collected from the opposite sides of the IZ) of the 16-channel array. This study is unable to examine the end-of-fiber effect and boundary conditions. In spite of its limitations, the present research explores the use of a relatively small number of electrodes for IZ estimation.

Acknowledgments

Conflicts of interest: None declared.
Funding: Davee Research Foundation and NIH R21NS093727.

References

[1] R. Merletti, D. Farina, M. Gazzoni, The linear electrode array: a useful tool with many applications, J Electromyogr Kines 13 (2003) 37–47.
[2] M.J. Zwarts, D.F. Stegeman, Multichannel surface EMG: basic aspects and clinical utility, Muscle Nerve 28 (2003) 1–17.
[3] B.G. Lapatki, J.P. van Dijk, I.E. Jonas, M.J. Zwarts, D.F. Stegeman, A thin, flexible multielectrode grid for high-density surface EMG, J. Appl. Physiol. 96 (2004) 327–336.
[4] M. Pozzo, A. Bottin, R. Ferrabone, R. Merletti, Sixty-four channel wearable acquisition system for long-term surface electromyogram recording with electrode arrays, Med. Biol. Eng. Comput. 42 (2004) 455–466.
[5] G. Rau, E. Schulte, C. Disselhorst-Klug, From cell to movement: to what answers does EMG really contribute? J Electromyogr Kines 14 (2004) 611–617.
[6] G. Drost, D.F. Stegeman, B.G.M. van Engelen, M.J. Zwarts, Clinical applications of high-density surface EMG: a systematic review, J Electromyogr Kines 16 (2006) 586–602.
[7] R. Merletti, A. Holobar, D. Farina, Analysis of motor units with high-density surface electromyography, J Electromyogr Kines 18 (2008) 879–890.
[8] R. Merletti, A. Botter, A. Troiano, E. Merlo, M.A. Minetto, Technology and instrumentation for detection and conditioning of the surface electromyographic signal: state of the art, Clin. Biomech. 24 (2009) 122–134.
[9] K. Saitou, T. Masuda, D. Michikami, R. Kojima, M. Okada, Innervation zones of the upper and lower limb muscles estimated by using multichannel surface EMG, J. Hum. Ergol. 29 (2000) 35–52.
[10] B.G. Lapatki, J.P. van Dijk, B.P.C. van de Warrenburg, M.J. Zwarts, Botulinum toxin has an increased effect when targeted toward the muscle's endplate zone: a high-density surface EMG guided study, Clin. Neurophysiol. 122 (2011) 1611–1616.
[11] A. Van Campenhout, G. Molenaers, Localization of the motor endplate zone in human skeletal muscles of the lower limb: anatomical guidelines for injection with botulinum toxin, Dev. Med. Child Neurol. 53 (2011) 108–119.
[12] J.E. Desmedt, Plasticity of motor unit organization studied by coherent electromyography in patients with nerve lesions or with myopathic or neuropathic diseases, Motor Unit Types, Recruitment and Plasticity in Health and Disease 9 (1981) 250–304.
[13] F. Jahanmiri-Nezhad, P.E. Barkhaus, W.Z. Rymer, P. Zhou, Innervation zones of fasciculating motor units: observations by a linear electrode array, Front. Hum. Neurosci. 9 (2015) 239.
[14] T. Masuda, H. Miyano, T. Sadoyama, The propagation of motor unit action potential and the location of neuromuscular junction investigated by surface electrode arrays, Electroencephalogr. Clin. Neurophysiol. 55 (1983) 594–600.
[15] T. Masuda, H. Miyano, T. Sadoyama, The position of innervation zones in the biceps brachii investigated by surface electromyography, IEEE (Inst. Electr. Electron. Eng.) Trans. Biomed. Eng. 32 (1985) 36–42.
[16] T. Masuda, T. Sadoyama, Distribution of innervation zones in the human biceps brachii, J. Electromyogr. Kinesiol. : official journal of the International Society of Electrophysiological Kinesiology 1 (1991) 107–115.
[17] R. Merletti, D. Farina, A. Granata, Non-invasive assessment of motor unit properties with linear electrode arrays, Electroencephalogr. Clin. Neurophysiol. Suppl. 50 (1999) 293–300.
[18] N. Ostlund, B. Gerdle, J. Stefan Karlsson, Location of innervation zone determined with multichannel surface electromyography using an optical flow technique, J. Electromyogr. Kinesiol. : official journal of the International Society of Electrophysiological Kinesiology 17 (2007) 549–555.
[19] J.M. Defreitas, P.B. Costa, E.D. Ryan, T.J. Herda, J.T. Cramer, T.W. Beck, An examination of innervation zone movement with increases in isometric torque production, Clin. Neurophysiol. 119 (2008) 2795–2799.
[20] J.M. DeFreitas, P.B. Costa, E.D. Ryan, T.J. Herda, J.T. Cramer, T.W. Beck, Innervation zone location of the biceps brachii, a comparison between genders and correlation with anthropometric measurements, J Electromyogr Kines 20 (2010) 76–80.
[21] L. Mesin, M. Gazzoni, R. Merletti, Automatic localisation of innervation zones: a simulation study of the external anal sphincter, J. Electromyogr. Kinesiol. : official journal of the International Society of Electrophysiological Kinesiology 19 (2009) e413–421.
[22] M. Barbero, R. Gatti, L. Lo Conte, F. Macmillan, F. Coutts, R. Merletti, Reliability of surface EMG matrix in locating the innervation zone of upper trapezius muscle, J Electromyogr Kines 21 (2011) 827–833.
[23] M. Barbero, C. Cescon, A. Tettamanti, V. Leggero, F. Macmillan, F. Coutts, R. Gatti, Myofascial trigger points and innervation zone locations in upper trapezius muscles, Bmc Musculoskel Dis 14 (2013).
[24] T.W. Beck, J.M. DeFreitas, M.S. Stock, Accuracy of three different techniques for automatically estimating innervation zone location, Comput. Methods Progr. Biomed. 105 (2012) 13–21.
[25] C. Cescon, Automatic location of muscle innervation zones from multi-channel surface EMG signals, IEEE International Workshop on Medical Measurement and Applications, MeMeA 2006, 2006, pp. 87–90.
[26] K. Ullah, C. Cescon, B. Afsharipour, R. Merletti, Automatic detection of motor unit innervation zones of the external anal sphincter by multichannel surface EMG, J. Electromyogr. Kinesiol. : official journal of the International Society of Electrophysiological Kinesiology 24 (2014) 860–867.
[27] F. Soares, M. De Andrade, A. Rocha, R. Merletti, Automatic Tracking of Innervation Zones Using Image Processing Methods, (2010).
[28] J.O. Street, R.J. Carroll, D. Ruppert, A note on computing robust regression estimates via iteratively reweighted least-squares, Am Stat 42 (1988) 152–154.
[29] K.E. Leffler, D.A. Jay, Enhancing tidal harmonic analysis: robust (hybrid L-1/L-2) solutions, Cont. Shelf Res. 29 (2009) 78–88.
[30] R. Plonsey, The active fiber in a volume conductor, IEEE (Inst. Electr. Electron. Eng.) Trans. Biomed. Eng. 21 (1974) 371–381.
[31] B.K. van Veen, H. Wolters, W. Wallinga, W.L. Rutten, H.B. Boom, The bioelectrical source in computing single muscle fiber action potentials, Biophys. J. 64 (1993) 1492–1498.
[32] J.A. Gonzalez-Cueto, P.A. Parker, Deconvolution estimation of motor unit conduction velocity distribution, IEEE (Inst. Electr. Electron. Eng.) Trans. Biomed. Eng. 49 (2002) 955–962.
[33] D. MacIsaac, D. Rogers, A. Bhandarkar, Simulating Myoelectric Signals with a Finite Length Model of Muscle, 29th Canadian Medical and Biological Engineering Conference, CMBEC'29), 2006.
[34] J.A. Gonzalez-Cueto, P.A. Parker, Deconvolution estimation of nerve conduction velocity distribution, IEEE (Inst. Electr. Electron. Eng.) Trans. Biomed. Eng. 49 (2002) 140–151.
[35] K.C. McGill, Z.C. Lateva, S.J. Xiao, A model of the muscle action potential for describing the leading edge, terminal wave, and slow afterwave, IEEE (Inst. Electr. Electron. Eng.) Trans. Biomed. Eng. 48 (2001) 1357–1365.
[36] B.R. Brooks, R.G. Miller, M. Swash, T.L. Munsat, W.F.N.R. Gr, El Escorial revisited: revised criteria for the diagnosis of amyotrophic lateral sclerosis, Amyotroph Lateral Sc 1 (2000) 293–299.
[37] J.Y. Moon, T.S. Hwang, S.J. Sim, S.I. Chun, M. Kim, Surface mapping of motor points in biceps brachii muscle, Annals of Rehabilitation Medicine 36 (2012) 187–196.
[38] J. Liu, S. Li, X. Li, C. Klein, W.Z. Rymer, P. Zhou, Suppression of stimulus artifact contaminating electrically evoked electromyography, NeuroRehabilitation 34 (2014) 381–389.
[39] D. Farina, C. Cescon, R. Merletti, Influence of anatomical, physical, and detection-system parameters on surface EMG, Biol. Cybern. 86 (2002) 445–456.
[40] D. Farina, R. Merletti, B. Indino, M. Nazzaro, M. Pozzo, Surface EMG crosstalk between knee extensor muscles: experimental and model results, Muscle Nerve 26 (2002) 681–695.
[41] Y. Liu, Y. Ning, S. Li, P. Zhou, W.Z. Rymer, Y. Zhang, Three-dimensional innervation zone imaging from multi-channel surface EMG recordings, Int. J. Neural Syst. 25 (2015) 1550024.
[42] A. Gallina, C.H. Ritzel, R. Merletti, T.M. Vieira, Do surface electromyograms provide physiological estimates of conduction velocity from the medial gastrocnemius muscle? J. Electromyogr. Kinesiol. : official journal of the International Society of Electrophysiological Kinesiology 23 (2013) 319–325.
[43] E.F. Hodson-Tole, I.D. Loram, T.M. Vieira, Myoelectric activity along human gastrocnemius medialis: different spatial distributions of postural and electrically elicited surface potentials, J. Electromyogr. Kinesiol. : official journal of the International Society of Electrophysiological Kinesiology 23 (2013) 43–50.